

Non-axisymmetric shapes of a rotating drop in an immiscible system

T. G. Wang, R. Tagg, L. Cammack, and A. Croonquist

Jet Propulsion Laboratory
 California Institute of Technology
 4800 Oak Grove Drive
 Pasadena, California 91109

Abstract

The non-axisymmetric shapes of a rotating drop in an immiscible system have been studied. Five basic families of shapes (axisymmetric, two-lobed, three-lobed, four-lobed, and toroidal) have been observed. The sequence (axisymmetric \rightarrow two-lobed \rightarrow three-lobed \rightarrow four-lobed \rightarrow toroidal) seems to be linked to increasing spin-up velocity. For the axisymmetric case, direct comparisons of experiments with the theory of a free rotating drop were surprisingly good — the equatorial area differs from theory by only 30%. Furthermore, the non-axisymmetric shapes are in good qualitative agreement with the theory, although the theory does not address the presence of an outer fluid.

Introduction

This paper describes the investigations of the dynamics of a rotating liquid mass under the influence of surface tension.

A large (~ 15 -cc) viscous liquid drop is formed around a disc and shaft in a tank containing a much less viscous mixture having the same density as the drop. This supporting liquid and the drop are immiscible. If the shaft and disc were not present, the drop would float freely in the surrounding medium and assume the shape of a sphere. With the drop attached and initially centered about the disc, the shaft and disc are set into rotation almost impulsively, reaching a final steady angular velocity within one-half to two revolutions. The drop deforms under rotation and develops into a variety of shapes depending on the shaft velocity. The process of spin-up, development, and decay (or fracture) to some final shape was common to all runs.

In this system, gravity is diminished at the expense of introducing a supporting liquid which is viscous and which may be entrained by the motion of the drop, thereby allowing angular momentum to be transferred from the drop. Nevertheless, comparison of this experiment's results to the theory of free rotating liquid drops is prompted by the fact that several novel families of drop shapes have been observed.

It is important to recognize that existing theory deals mainly with equilibrium shapes and their stability, while the drop in this experiment is undergoing a far more complicated process. The shape of a liquid drop spun on a shaft and supported by another liquid is very much a dynamical problem. A proper understanding of the results will only come with a dynamical analysis which succeeds in explaining the growth and decay with time of the various drop shapes.

Theory

The theory of the equilibrium shapes of rotating fluids began with investigations by Newton on the shape of the rotating earth, and the extensive theory that ensued was that of a free fluid held together by self-gravitation. An equilibrium figure for rotating liquid drops held together by surface tension was not demonstrated until more than seventy years later when Rayleigh⁽¹⁾ investigated droplets symmetric about the rotation axis (see also Appell⁽²⁾). The stability of the simple axisymmetric shapes awaited study by Chandrasekhar⁽³⁾.

Swiatecki⁽⁴⁾ fits the problem of a liquid drop held together by surface tension into a broader scheme in which fluid masses may, in addition to having surface tension, be self-gravitating and/or possess a uniform density of electric charge. The astrophysical problem of the stability of rotating, self-gravitating stellar masses, and the problem of the fissionability of rotating, uniformly-charged "liquid drop" nuclei in nuclear physics, are thus unified with the problem of equilibrium shapes and stability of ordinary liquid drops.

Confining discussion to the case of surface tension forces only, it is necessary to define some of the parameters used to describe a free liquid drop in solid body rotation. The "free" drop is actually assumed to be contained within another fluid (for example, an atmosphere of gas) which rotates at the same angular velocity. The drop has density ρ_D and

ORIGINAL PAGE IS
OF POOR QUALITY

rotates with angular velocity Ω . The outer fluid has density $\rho_F < \rho_D$. The equilibrium shape of the drop must satisfy the equation: ⁽⁵⁾

$$\Delta p_o + \frac{1}{2} \Delta \rho \Omega^2 r_1^2 = \sigma \nabla \cdot \hat{n}, \quad (1)$$

subject to the constraint that the drop have a fixed volume. $\Delta p_o \equiv P_{D_o} - P_{F_o}$ is the difference in pressures on the axis of rotation inside and outside the drop, $\Delta \rho = \rho_D - \rho_F$ is the density difference, r_1 is the radius perpendicular to the axis of rotation and extending to the drop's surface, σ is the interfacial tension, and \hat{n} is normal to the surface ($-1/2 \nabla \cdot \hat{n}$ is the local mean curvature).

If the density difference $\Delta \rho$ is zero, the effect of rotation (i.e., the centrifugal term $(1/2) \Delta \rho \Omega^2 r_1^2$) is completely removed and the shape satisfying Equation (1) would be a perfect sphere. In this experiment, however, the drop was rotated differentially with respect to the outer fluid, giving rise to the analogous centrifugal term $(1/2) \rho (\Delta \Omega)^2 r_1^2$; this approach must suffer the effects of viscous drag and entrainment of the outer fluid. Some basis for comparison with the "free" drop system is preserved by making the outer fluid two orders of magnitude less viscous than the drop, and the experimental time short. Thus, a minimum amount of angular momentum transfers across the interface during the critical part of the experiment.

Returning to the free drop theory: Brown ⁽⁵⁾ rewrites Equation (1) in a dimensionless form

$$Ha_o = K + 2 \Sigma \left(\frac{r_1}{a_o} \right)^2, \quad (2)$$

where $H \equiv 1/2 \nabla \cdot \hat{n}$ is the local mean curvature, a_o is the radius of a sphere having the same volume as the drop, and the parameters Σ and K are the rotational bond number and dimensionless reference pressure defined by:

$$\Sigma \equiv \frac{\Omega^2 \Delta \rho a_o^3}{8\sigma}, \quad (3)$$

$$K \equiv \frac{\Delta p_o a_o}{2\sigma}. \quad (4)$$

The axisymmetric and non-axisymmetric sequences excluding toroidal shapes may also be represented by a plot of the normalized equatorial area against Σ . (Figure 1).

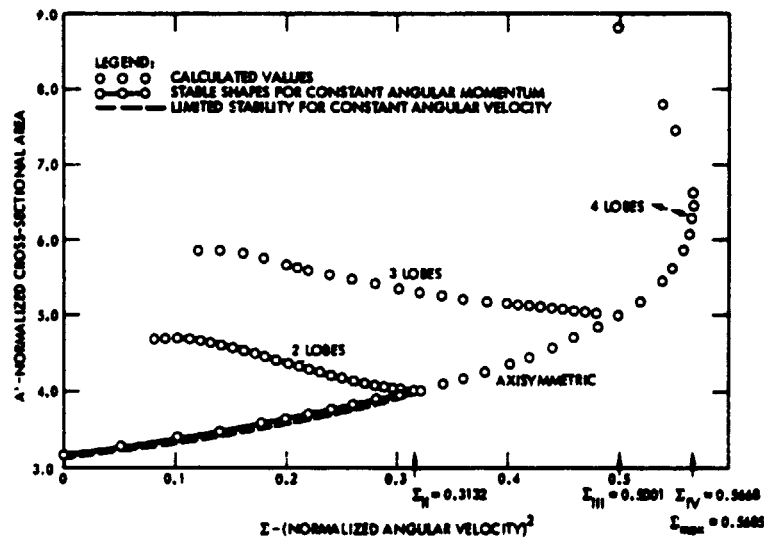


Figure 1. Calculated Equilibrium Shapes (from data reported by Brown ⁽⁵⁾, supplemented by Chandrasekhar ⁽³⁾ and Ross ⁽⁷⁾).

Experiment

The immiscible tank (see Figure 2) in which the drop is buoyantly supported and rotated consists of a Lucite cylinder which in turn is contained in a cubical outer tank. Cylindrical symmetry about the axis of rotation is thus obtained while lens-like distortion of the drop inside the cylindrical tank is minimized by the parallel-sided geometry of the outer tank and the water circulating between it and the inner tank.

The circulating water is pumped into the system from a constant-temperature bath with a 15-liter capacity. By this means we are able to control the temperature of the system to within $.01^{\circ}\text{C}$ or better, such control is one of the most critical factors in the performance of the experiment.

The fluids we used in this experiment are silicone oil (Dow Corning 200,100 centistoke) for the drop, and a 3 to 1 water/methanol mixture for the host. The physical properties of the mixture are highly dependent on the temperature. Therefore, the equilibrium positions of the drop are extremely sensitive to the temperature gradient as shown in Figure 3.

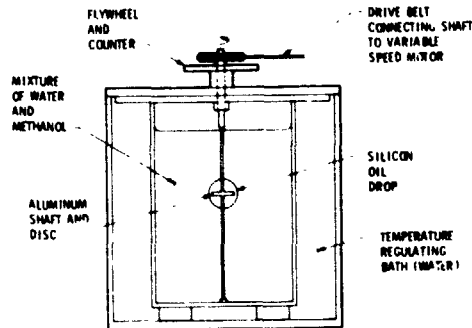


Figure 2. Immiscible System Apparatus

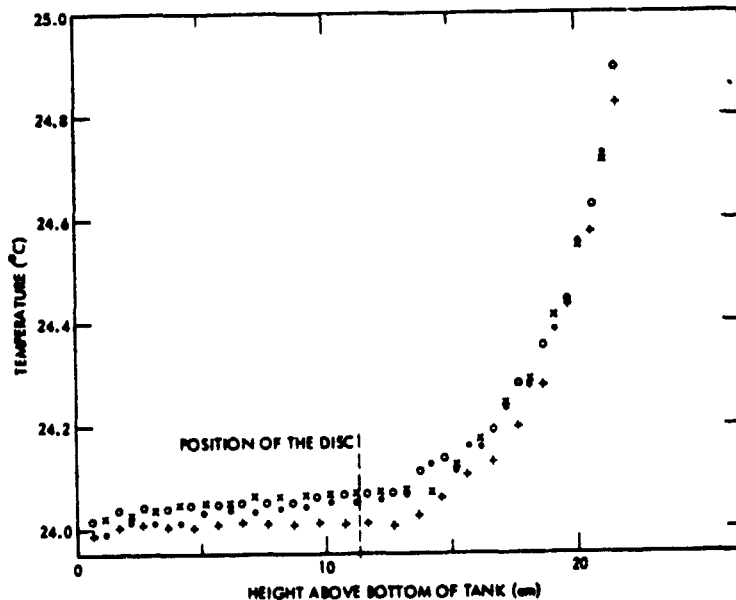


Figure 3. Temperature Profile of the Neutral Buoyancy Tank (Measurements made by Tom Chuh).

The shapes of rotating spheroids and the fluid flows are recorded on a camera (Milliken DBM-55) and digitized on a Vanguard Motion Analyzer. The flow visualization for inside the drop is accomplished by forming tracer particles out of the water/methanol mixture of different densities and vice versa for flow outside the drop.

Results and Discussion

Five basic families of shapes are observed.^(7,8) They are axisymmetric, two-lobed, three-lobed, four-lobed, and toroidal. Additionally, the off-axis single lobe is the final shape for all experimental runs except those in which the drop undergoes fracture. These shapes are shown in Figures 4-10.

Apart from the axisymmetric shapes at slow rotation rates, the three-lobed family was the easiest to obtain. This fact was due in part to the particular drop volumes and shaft dimensions used in this experiment. The ease with which three-lobed shapes are generated is nevertheless remarkable; even in an early, very crude 1/4-scale version of the experiment, three-lobed shapes were readily obtained.

Two-lobed shapes, which develop for slower shaft velocities (<2 rps), may be harder to obtain because the decay processes which cause the drop to form into an asymmetric single lobe may set in before the drop can develop symmetric lobes. Four-lobed shapes, on the other hand, are obtained at generally higher shaft velocities (~ 4 rps) than the three-lobed shapes; when asymmetries develop in the drop at these angular velocities, fracture usually results.

During the decay of higher non-axisymmetric modes, one-lobe generally rotates faster than the others, eventually catching up and joining with the lobe preceding it. Thus, three converge into two and two into one. This is not surprising; the mass of the drop is never equally distributed among the lobes; so one lobe is smaller and suffers less drag by the surrounding fluid. The presence of drag is immediately apparent from the pinwheel appearance of all of the lobed shapes, with the lobes curving backwards against the direction of rotation.

A further effect, attributed to the motion of the outer fluid, appears in many runs in which two- and three-lobed shapes are produced; in the course of the drop's development, the drop rises and becomes sessile on top of the disc (i.e., it only contacts the upper surface of the disc and shaft). Three-lobes decay to two-lobes which are sessile (Figure 13) and often persist for many seconds before decaying to a single lobe (also sessile). This rising of the drop occurs even when the level of exact density matching is below the disc by, for example, two centimeters. Furthermore, above a rather well-defined shaft velocity midway in the range of velocities producing three-lobed shapes, a different effect occurs. The three-lobed drop still decays to a two-lobed one but with one lobe above the disc and the other below, i.e., the drop is tilted (Figure 14). This appears to be a very stable geometry which can persist for minutes.

Only a few instances of the toroidal shape have been observed with this system. Nevertheless, striking examples have been photographed of the formation of a torus and its subsequent highly symmetric fracture into three or four large drops and a corresponding number of small satellite drops (Figures 10 through 12). The sequence (axisymmetric - two lobed - three lobed - four lobed - toroidal) seems to be linked to increasing spin-up velocity.

ORIGINAL PAGE
BLACK AND WHITE PHOTOGRAPH

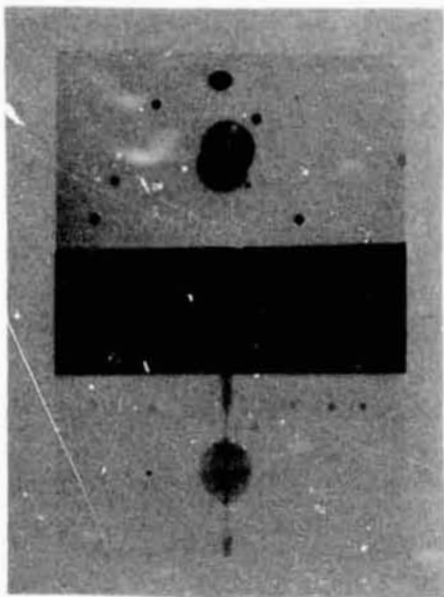


Figure 4. Drop At Rest. Note internal trace drops and external satellite drops.

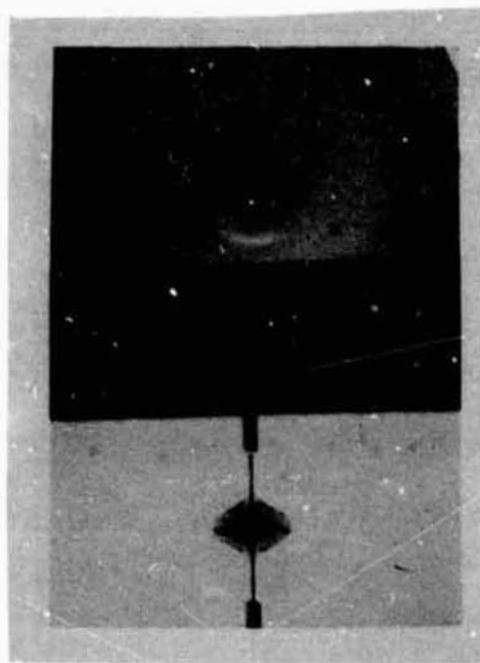


Figure 5. Axisymmetric Oblate Drop. (Shaft angular velocity = 0.8 rps).

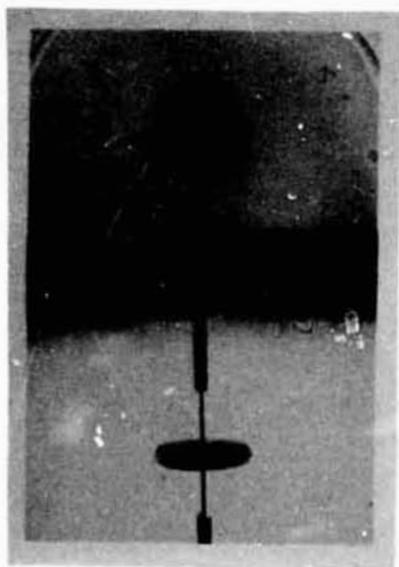


Figure 6. Axisymmetric Biconcave Drop (Shaft angular velocity = 1.3 rps), drop is still spinning up)

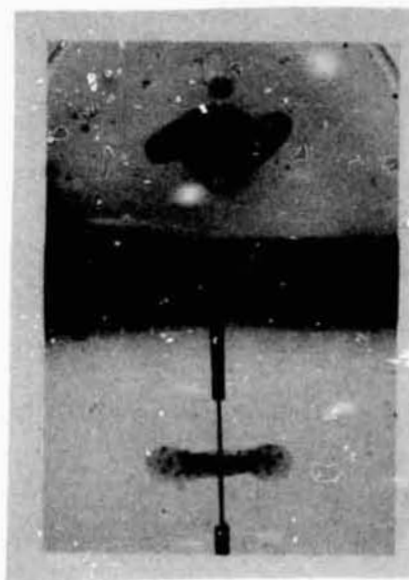


Figure 7. Two-lobed shape (Shaft angular velocity = 1.8 rps).

ORIGINAL PAGE
BLACK AND WHITE PHOTOGRAPH

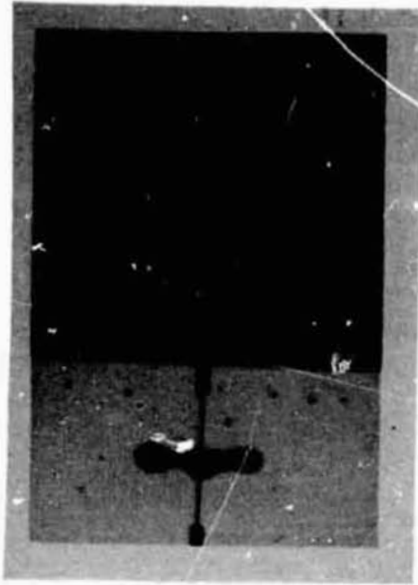


Figure 8. Three-lobed Shape
(Shaft angular velocity = 2.0 rps)



Figure 9. Four-lobed Shape
(Shaft angular velocity = 3.6 rps)

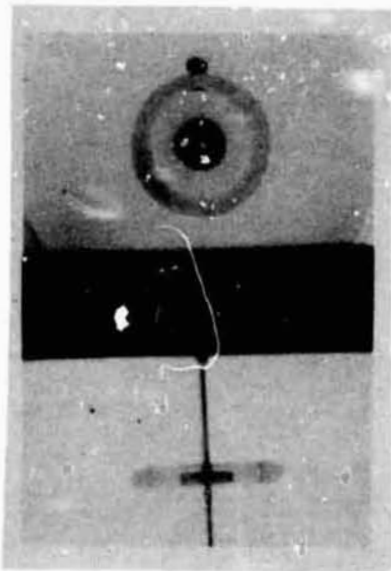


Figure 10. Torus (Shaft angular
velocity = 4.8 rps)

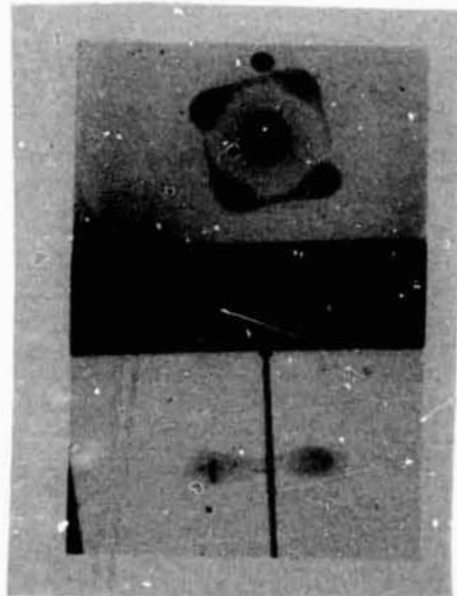


Figure 11. Break Up of Torus
(Shaft is not rotating)

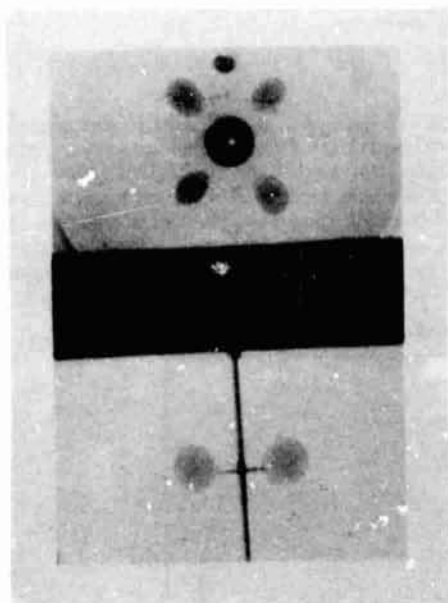


Figure 12. Break Up of Torus
(Shaft is not rotating)



Figure 13. Single Lobe
(Ultimate decay shape)

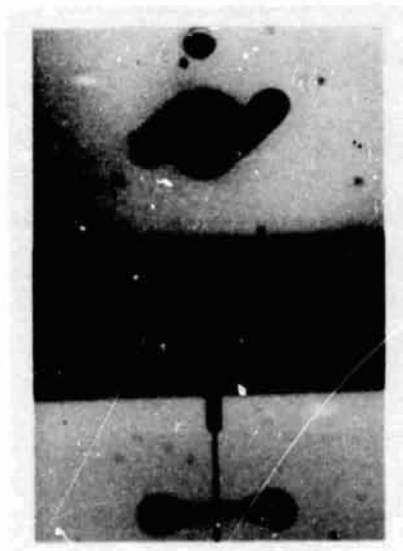


Figure 14. Sessile Two-Lobed
Shape (The results of decay
from a three-lobed shape; shaft
is not rotating)



Figure 15. Tilted Two-Lobed
Shape (Decay route for three-
lobed shapes)

The comparisons between the shapes that we observed and the calculations by Brown⁽⁵⁾, Chandrasekhar⁽³⁾, and Ross⁽⁷⁾ are given in the following section.

A. Axisymmetric shape

The quantities which are determined for the axisymmetric shapes are a , the equatorial radius of the rotating drop, and Ω , the drop's angular velocity. From a the normalized cross-sectional area $A' = \pi a^2 / a_0^2$ is calculated, while Ω yields the dimensionless parameter Σ , ρ is the density of the oil and σ is the interfacial tension between the oil and mixture. a_0 is computed from the calculated drop volume. The experimental axisymmetric values are determined from the maximum drop deformation for a given rotation velocity. The experimental values are presented in Figure 16. As Σ increases, the axisymmetric shapes become less stable with respect to the $n=1$ perturbation. Thus, no reliable data are available beyond the region where $\Sigma = 0.4$.

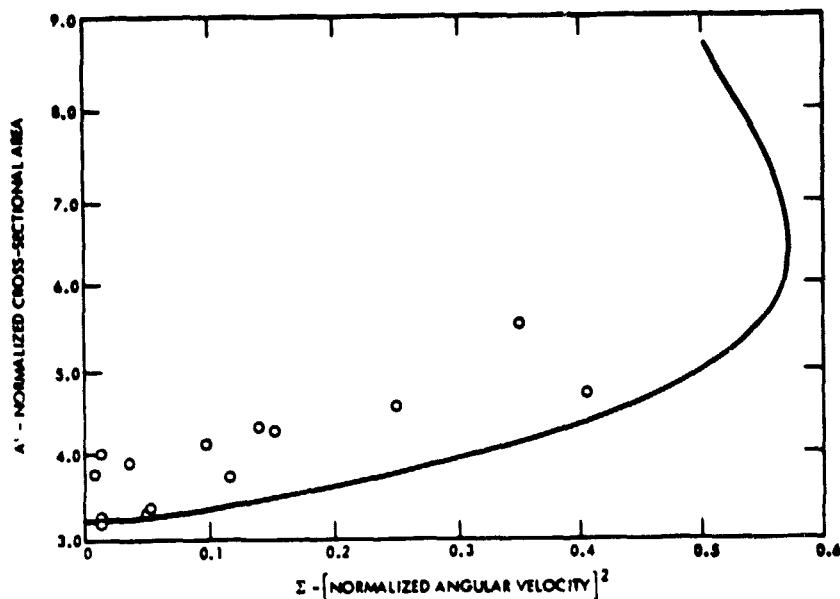


Figure 16. Experimental Results for Slowly Rotating Axisymmetric Drops. Theoretical Curve From Free Drop Calculations. 3,5,6

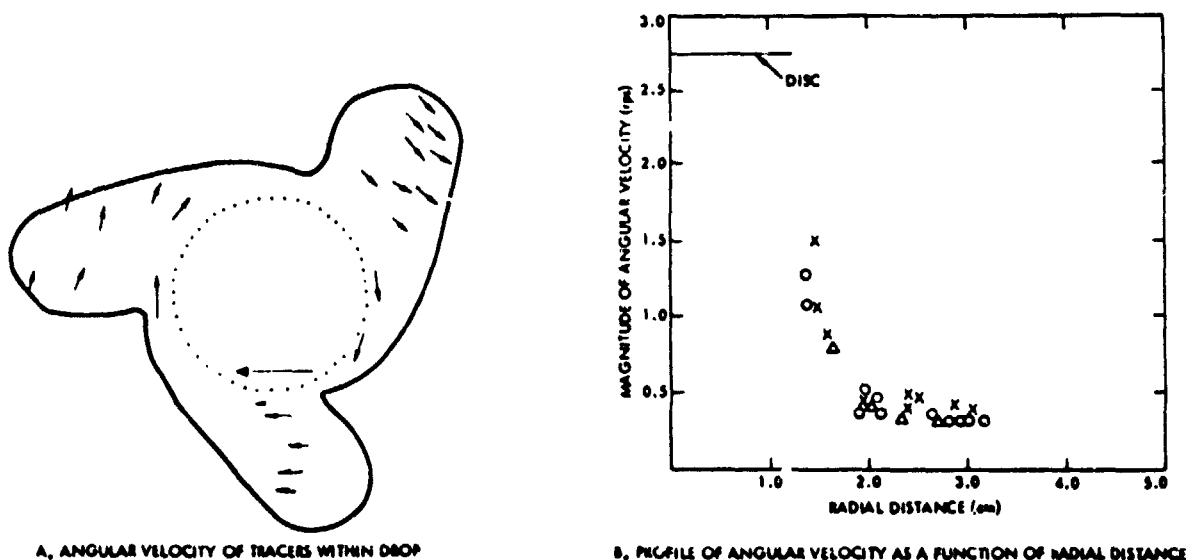


Figure 17. Angular Velocity Distribution for Three-Lobed Shape;
 Drop = 0.33 rps and Shaft = 2.74 rps

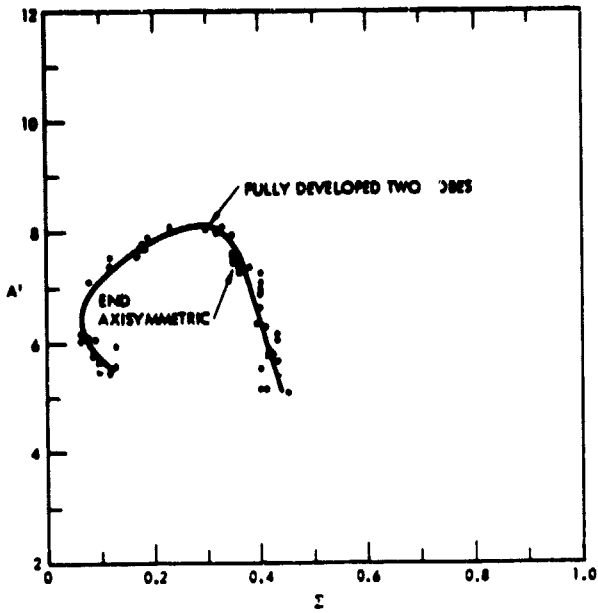


Figure 18. A' versus Σ for a Two-Lobe Run. (A' is the normalized equatorial area and Σ is proportional to the square of the angular velocity).

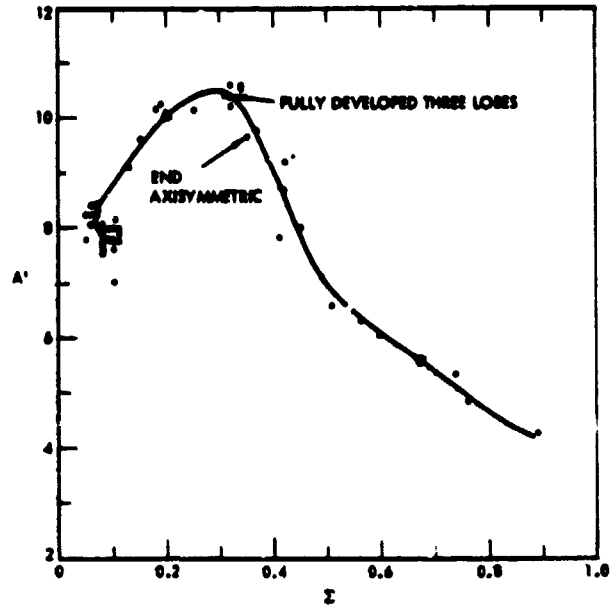


Figure 19. A' versus Σ for Three Lobe Run.

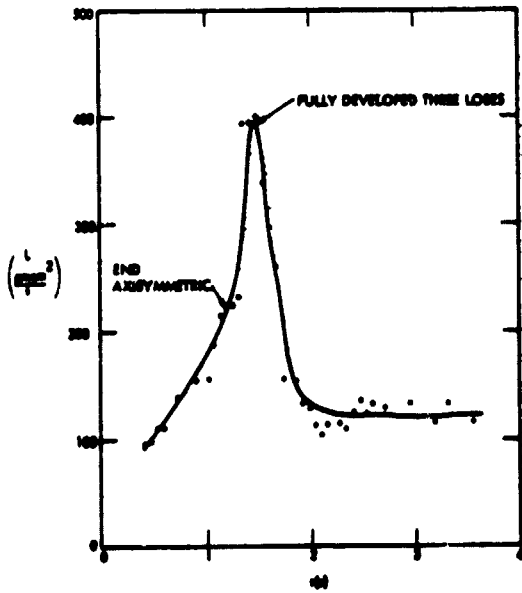


Figure 20. A' versus Σ for a Four Lobe Run.

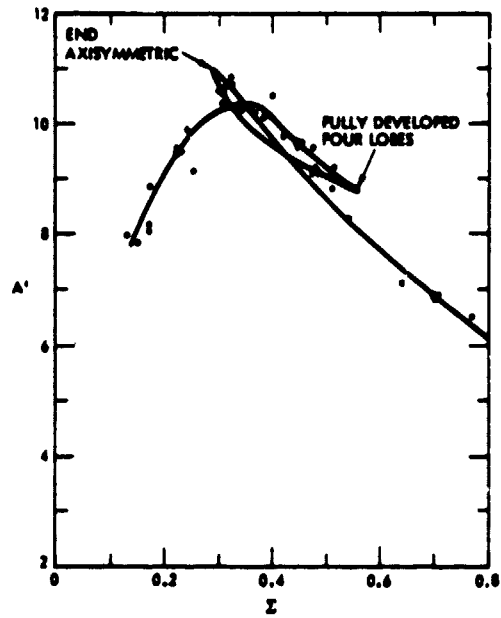


Figure 21. Angular Momentum versus Time for a Three Lobe Run.

B. Non-axisymmetric shapes

Figure 17 shows velocity-profile data for a three-lobed shape. The existence of shear close to the disc is clearly demonstrated. It is also seen, that at a position away from the disc where 90 percent of the mass is located, a reasonably constant angular velocity exists. It is the measurement of this velocity which serves as the Ω value for determining Γ for a given drop shape. However, the justification of this procedure is likely to break down during the initial spin up of the drop.

Figures 18-20 show graphs of the results of A/a_0^2 versus Γ for the drops which developed to two-lobed, three-lobed, and four-lobed shapes.

The direction in which the A' versus Γ graphs was traveled, the time is indicated on each graph. In each run, the drop remains axisymmetric for a time prior to developing into its lobed shape.

By looking at the A' -versus- Γ graphs of the three- and four-lobed runs, it can be seen that the curves occupy the same domain. This fact suggests the possibility that bifurcation points for the four-lobed and three-lobed shapes are close, and the three-lobed shape is more stable. As a result, the three-lobed shape occurred more frequently than the four-lobed shape.

The four-lobed curve of A' versus Γ has a rebound that is either nonexistent or not as profound in the three- and two-lobed runs.

In all runs, the angular momentum increases initially, reaches a peak, and then decreases. The shaft angular velocity is constant in the critical region, before and after the lobes have fully developed. (See Figure 21).

CONCLUSIONS

Shapes of a rotating spheroid, have been observed and recorded in this experiment. These include the flattening of slowly rotating drops and the generation of toroidal and lobed shapes at higher rotation rates. Using data recorded on movie film, the development and decay of the rotating shapes were studied for the first time. The neutrally buoyant tracer droplets allowed us to study the dynamics of the behavior, the secondary flow generated by the rotation, the interaction between the drop and the host liquid, and the coupling between the shaft and disc and the drop.

For slowly rotating axisymmetric drops, direct comparisons of experiment with the theory of a free rotating drop were possible. The agreement was surprisingly good; the qualitative shape of the equatorial-area-versus- Γ curves were similar, only differing from theory by 30%. This is remarkable because the theory does not address the presence of an outer fluid. The generation and study of axisymmetric equilibrium shapes for higher rotation rates is difficult, because of the presence of the more stable off-axis single lobed shape. This mechanism, axisymmetric shapes decay into single lobed shape, prohibited us from extracting from the data the exact location of the bifurcation points between families of equilibrium shapes.

When generating $n \geq 2$ lobed drops in a controlled manner, primarily two- and three-lobed shapes were obtained. The latter had not been observed before. The study of equilibrium configurations of these lobed shapes is made difficult by the presence of the outer fluid; as soon as the lobes occur, the interaction between the drop and the host liquid increases significantly and generates large secondary flows. The accelerated transfer of angular momentum from the drop in the lobed configurations gives rise to decay routes in which one lobe slows and is absorbed by the one trailing it; this process continues until there is only an arm left. There were two exceptional types of decay in which either the whole drop would lift up (independently of the neutral buoyancy level) and become sessile on the disc, or would form a slanted drop; in both of these two cases, the shapes were very stable and long-lived. The behavior of lobed shapes was not easily compared to the free drop theory. The study of the angular velocities and momenta demonstrated that the development of the various lobed shapes takes similar paths, but no evidence was found for the location of branch points between axisymmetric and triaxial behavior.

At present, no framework exists for describing the dynamics of a drop rotating in another liquid. It is the authors' hope that the various phenomena observed and described in the course of this work will stimulate one.

REFERENCES

1. Rayleigh, Lord, "Equilibrium of Revolving Liquid Under Capillary Forces," *Phil. Mag.* 28, 161 (1914).
2. Appell, P., Traite de Mecanique Rationelle, Vol. 4, Pt. 1, Chapt. IX, Gauthier-Villars, Paris (1932).
3. Chandrasekhar, S., "The Stability of a Rotating Liquid Drop," *Proc. Roy. Soc. (London)*, 286, 1 (1965).
4. Swiatecki, W.J., "The Rotating, Charged or Gravitating Liquid Drop, and Problems in Nuclear Physics and Astronomy," *Ibid.*, p 52.
5. Brown, R., "The Shape and Stability of Three-Dimensional Interfaces," PhD Thesis, University of Minnesota (Minneapolis, MN, 1979).
6. Ross, D.K., "The Shape and Energy of a Revolving Liquid Mass Held Together by Surface Tension," *Aust. J. Phys.* 21, (1968), p. 823.
7. Tagg, R., Cammack, L., Croonquist, A., and Wang, T.G., "Rotating Liquid Drops; Plateau's Experiment Revisited," *Jet Propulsion Laboratory, Publication 80-66* (1980).
8. Tagg, R., and Wang, T.G., "The Shapes of Rotating Liquid Drops Neutrally Buoyant in Another Liquid," *Bull. Am. Physical Soc.* (1978).